Hindawi
Advances in Civil Engineering
Volume 2019, Article ID 4546324, 12 pages
https://doi.org/10.1155/2019/4546324

Research Article

Prediction Method for Overconsolidation Ratio of Marine Soft Soil Based on the Piezocone Penetration Tests

Yanbin Fu,[1,2] **Sizhan Zhang**,[1] **Guiyang Lv**,[1] **and Kaihang Han**[1,2]

[1]*College of Civil and Transportation Engineering, Shenzhen University, Shenzhen 518060, China*
[2]*Underground Polis Academy of Shenzhen University, Shenzhen 518060, China*

Correspondence should be addressed to Kaihang Han; hankaihang@bjtu.edu.cn

Received 24 April 2019; Accepted 7 July 2019; Published 30 July 2019

Academic Editor: Salvatore Grasso

Because of the strong structural and sensitive behavior, the properties of marine soft soil change greatly when subjected to external disturbances, which leads to great difficulty in reflecting its real mechanical properties in the laboratory soil tests. The piezocone penetration test (CPTU) is one of the main technologies for in situ testing of geotechnical engineering. CPTU has the advantages of being fast and convenient, no sampling, low disturbance to soil, large amount of data, and reliable testing. The determination of the overconsolidation ratio (OCR) based on the CPTU results can solve the problems of soil disturbance and stress release, which occur during the consolidation test in the laboratory. However, there are still some problems such as lack of strict theoretical analysis of penetration mechanism and incomplete interpretation theory of in situ test parameters of CPTU. In this paper, the CPTU cone head is assumed to be hemispherical considering the penetration mechanism of CPTU. Moreover, the compaction modes of the CPTU probe penetrating into soil are adopted as spherical and cylindrical cavity expansion modes, respectively. The ultimate expansion pressures of the probe penetrating into soil under the spherical and cylindrical cavity expansion modes are first obtained by virtue of the theory of cavity expansion. Then, two prediction methods for OCR considering the roughness and penetration rate of the cone are proposed by combining the ultimate expansion pressures of the probe penetrating the approximate closed solution of cavity expansion in the modified Cambridge model, which is suitable for predicting the OCR of marine soft clay. Finally, to verify the reliability of the two proposed prediction methods, comparisons with the in situ CPTU tests of marine soft clay in two coastal areas and two existing prediction methods are made. The comparison results show that predictions of OCR of marine soft clay in this paper are close to Wayne's method and more accurate than Chanmee's method since the factors such as cone roughness and penetration rate are considered in the new proposed prediction methods. In order to improve the applicability in different cases of the OCR predictions, the average values of the two proposed methods are recommended as the reference value for the OCR of marine soft soil.

1. Introduction

Overconsolidation ratio (OCR) of soils is one of the factors that affect the strength, stress-strain, and compressibility of soils. It is also an important parameter for foundation settlement calculation and slope stability analysis. In the previous studies on the overconsolidation ratio, most of the research results are based on heavily overconsolidated soil. There are few studies on normal consolidation and lightly overconsolidated marine soft clay, and there is still no unified understanding of the overconsolidation ratio (OCR) of coastal soft clay. The overconsolidation ratio is usually obtained by the laboratory consolidation test with field soil samples. Because it is difficult to overcome the problems of stress release and soil disturbance during the sampling process, the test results can hardly reflect the real situation of foundation soil. However, because of the structural and sensitive behavior of marine soft soil, its engineering properties are poor. When disturbed by external disturbances, its properties change greatly. Therefore, it is difficult to accurately calculate the overconsolidation ratio of marine soft soil by conventional methods.

The piezocone penetration test (CPTU), with the advantages of being fast and convenient, no sampling, low disturbance to soil, large amount of data, and reliable testing, is one of the main technologies for in situ testing of geotechnical engineering, which is applied to determine the parameters of geotechnical engineering [1–4]. Determining the preconsolidation pressure or overconsolidation ratio of soil by the CPTU results can solve the problems of stress release and disturbance of soil samples during laboratory consolidation test, reflect the stress history of soil more truly, and provide a reference for the correct evaluation of site engineering geological conditions [5]. However, in the process of CPTU penetration into soil, the deformation and failure of soil is very complex. When the penetration process is regarded as the quasistatic process, the solution of the whole problem should satisfy the equilibrium equation, the geometric equation (large deformation), the boundary conditions of force and displacement, and the constitutive relationship of soil. Due to the complexity of the problem, it is very difficult to obtain an accurate solution. On the one hand, the theoretical foundation of the CPTU penetration mechanism is not so in-deep, and different theories correspond to different interpretation methods. On the other hand, its application is affected by soil type, in situ stress state, probe roughness, boundary conditions, and drainage conditions, which makes theoretical interpretation difficult and fail to guarantee the reliability of test parameters. Then, the interpretation of test parameters is affected.

At present, there are nearly 20 methods for determining the preconsolidation pressure or overconsolidation ratio (OCR) based on the CPTU test results [6]. These methods can generally be divided into empirical methods and theoretical methods. Mayne [7] and Wroth [8] proposed an empirical calculation formula for calculating OCR based on normalized net cone tip resistance, but the method relies on the nature of soil and its correlation is lower in cracked clay layers [9]. Mayne [7] established an empirical relationship between normalized excess pore water pressure and OCR through a large number of experiments. The empirical parameters in this method are derived from normal consolidated soil or slightly overconsolidated soil. Also, it is not applicable in heavily overconsolidated soil or fractured clay where the excess pore water pressure is small, even negative [10]. Houlsby [11] established an OCR empirical calculation method based on normalized effective tip resistance calculation, which has certain applicability for general sedimentary soils, but for normally consolidated soft soils, the method has a certain degree of dispersion. Mayne [12] combined the theory of cavity expansion in ideal elastoplastic soil with the critical state theory and proposed a theoretical calculation method of OCR in 1991, which is expressed as equation follows:

$$\mathrm{OCR} = 2\left[\frac{1}{1.95M+1}\left(\frac{q_t - u_2}{\sigma'_{vo}}\right)\right]^{(1/\Lambda)}, \tag{1}$$

where M is the slope of the critical state line, $M = 6\sin\varphi'/(3-\sin\varphi')$, φ' is the effective stress friction angle, σ'_{vo} is the effective overburden stress, Λ is the plastic volumetric strain ratio, $\Lambda = 1-\kappa/\lambda$, κ is the isotropic swelling index, and λ is the isotropic compression index. Although the method does not consider the influence of roughness, strain rate, initial stress state, anisotropy and stress ratio between the probe and the soil, the method breaks through the limitation of the clay type and is extensively applied. Figure 1 shows the CPTU probe entity and schematic diagram.

In recent years, some scholars have proposed some modified methods for predicting OCR. Zhang et al. [13] considered the penetration of piezocone as the ultimate internal pressure required in expanding a spherical cavity. Based on the solution of a spherical cavity expansion described with the modified cam clay, a modified approach to determine the OCR from CPTU was proposed. Chanmee et al. [14] combined the undrained shear strength of the modified Cambridge model with the undrained shear strength based on the net cone tip resistance to determine the OCR of soil by the iteration convergence method, which is expressed as follows:

$$\mathrm{OCR} = \left(\frac{q_t - \sigma_{vo}}{N_{kt}}\right)^{1/\Lambda}\left(\frac{2^{1+\Lambda}}{Mp'}\right)^{1/\Lambda}\left(\frac{M^2}{M^2+\eta^2}\right), \tag{2}$$

where N_{kt} is the cone bearing factor, σ_{vo} is the total stress in the vertical direction, Λ is the plastic volumetric strain ratio, M is the slope of the critical state line, p' is the average effective stress, and η is the ratio of stress, which is the function of OCR.

As mentioned above, empirical prediction formulas for predicting OCR are fitted by regression from a large number of in situ test results; however, they have strong geographical limitations and are suitable for the special cases. The classical theoretical prediction formula is relatively simple and breaks through the limitation of clay types, but fewer factors are considered. Some important parameters such as penetration rate, friction between cone and soil, and large deformation are not considered in classical theoretical prediction formulas.

In this paper, the CPTU cone head is assumed to be hemispherical considering the penetration mechanism of CPTU. And the compaction modes of the CPTU probe penetrating into soil are adopted as spherical and cylindrical cavity expansion modes, respectively. Two prediction methods for OCR considering the roughness and penetration rate of cone are proposed by combining the ultimate expansion pressures of probe penetrating with the approximate closed solution of cavity expansion in the modified Cambridge model, which is suitable for predicting the OCR of marine soft clay. Finally, to verify the reliability of the two proposed prediction methods, comparisons with the in situ CPTU tests of marine soft clay in two coastal areas and two existing prediction methods are carried out.

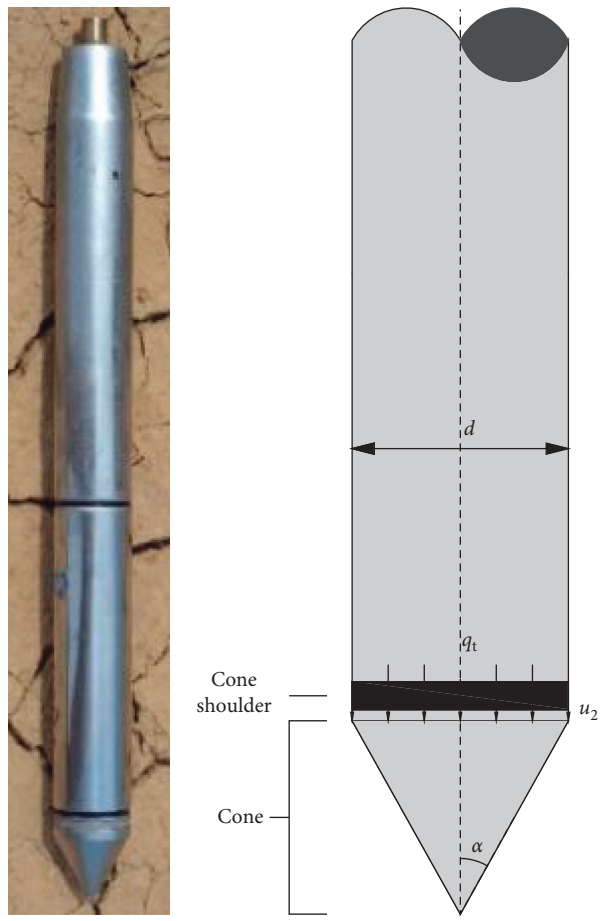

(a) (b)

Figure 1: (a) CPTU probe entity and (b) schematic diagram.

2. Proposal of Methods for Predicting OCR of Marine Soft Soil

2.1. Ultimate Expanding Pressure of Probe Penetrating. The expanding process of the CPTU probe penetrating into the soil can be considered as the one-dimensional boundary value problem of the small cavity expansion in the geomechanics. The ultimate expanding pressure is derived by the cavity expansion theory, and then, the expression of the cone tip resistance is determined. Figure 2 shows cavities before expansion and in expansion conditions, and it is assumed that the initial radius of the cavity is a_0 and the initial expanding pressure is σ_0. For the penetration process of the CPTU cone, it is considered to be a cavity expansion process with an initial radius of $a_0 = 0$. Compressive stresses and strains are taken as positive. The cavity expands to a radius of a_x as the internal cavity pressure increases from σ_0 to σ_{ax}. Correspondingly, an element initially at a radial distance r_0 from the centre of the cavity moves to a new radial position r from the centre, where the radial stress is σ_r and the circumferential stress is σ_θ, resulting in a displacement $u_r = r - r_0$. Two basic assumptions are made. Before yielding, the soil is assumed to be elastic while after yielding, the soil obeys the modified Cambridge model. The soil is an isotropic geotechnical medium.

2.1.1. Equilibrium Conditions and Boundary Conditions. Based on the above assumptions, cylindrical cavity expansion corresponds to the axisymmetric problem, while spherical cavity expansion corresponds to the spherical symmetry problem. For the plastic zone and the elastic zone, the soil element at the centre point of the cavity is r, which is obtained by the following equilibrium equation:

$$\frac{\partial \sigma_r}{\partial r} + m\frac{\sigma_r - \sigma_\theta}{r} = 0. \tag{3}$$

The solutions for the spherical and cylindrical cases can be developed together by assigning $m = 1$ for the cylindrical case and $m = 2$ for the spherical case. The total mean stress p and the deviator stress q for the cylindrical and spherical cases can be expressed as

$$p = \frac{\sigma_r + m\sigma_\theta}{1 + m}, \tag{4a}$$

$$q = \frac{\sqrt{m+2}}{2}\left(\sigma_r - \sigma_\theta\right). \tag{4b}$$

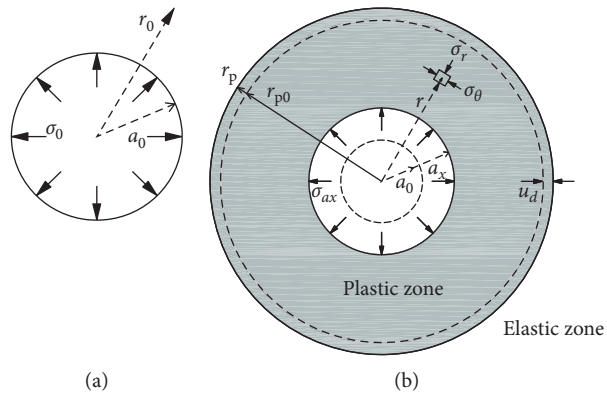

Figure 2: Schematic diagram of cavity expansion. (a) Cavity before expansion. (b) Cavity in expansion.

2.1.2. Elastic Analysis. The increment of radial and circumferential strains ($\Delta\varepsilon_r$ and $\Delta\varepsilon_\theta$) can be related to the increment of radial displacement Δu_r:

$$\Delta\varepsilon_r = -\frac{d\Delta u_r}{dr}, \tag{5a}$$

$$\Delta\varepsilon_\theta = -\frac{\Delta u_r}{r}. \tag{5b}$$

Since the soil was initially acted upon by σ_0, the increment of radial stress $\Delta\sigma_r$ and the increment of circumferential stress $\Delta\sigma_\theta$ can be calculated as follows:

$$\Delta\sigma_r = \sigma_r - \sigma_0, \tag{6a}$$

$$\Delta\sigma_\theta = \sigma_\theta - \sigma_0. \tag{6b}$$

Using Hooke's law, the increments of radial strain and circumferential strain around a cavity can be related to the stresses as follows:

$$\Delta\varepsilon_r = \frac{1-\nu^2(2-m)}{E}\left[\Delta\sigma_r - \frac{m\nu}{1-\nu(2-m)}\Delta\sigma_\theta\right], \tag{7a}$$

$$\Delta\varepsilon_\theta = \frac{1-\nu^2(2-m)}{E}\left\{[1-\nu(m-1)]\Delta\sigma_\theta - \frac{\nu}{1-\nu(2-m)}\Delta\sigma_r\right\}. \tag{7b}$$

Moreover, the relevant boundary conditions of radial stress at a_x and infinity are

$$\begin{cases} \sigma_{r(a_x)} = \sigma_{ax} + \sigma_0, \\ \lim\limits_{r\longrightarrow\infty} \sigma_r = \sigma_0. \end{cases} \tag{8}$$

Therefore, the solutions of stress and displacement in elastic region can be obtained by virtue of equations (4a)–(8) [15]:

$$\sigma_r = \sigma_0 + (\sigma_{ax} - \sigma_0)\left(\frac{a_x}{r}\right)^{m+1}, \tag{9a}$$

$$\sigma_\theta = \sigma_0 - \frac{1}{m}(\sigma_{ax} - \sigma_0)\left(\frac{a_x}{r}\right)^{m+1}, \tag{9b}$$

$$u_r = \frac{(\sigma_{ax} - \sigma_0)}{2mG}\left(\frac{a_x}{r}\right)^{m+1} r, \tag{9c}$$

where G is the shear modulus, defined as $E/2(1+\nu)$, and ν is Poisson's ratio.

2.1.3. Plastic Analysis. Assuming that the radius of elastic-plastic boundary is r_p, the solutions of stress and displacement at the elastic-plastic boundary can be expressed as follows, by virtue of equations (9a)~(9c):

$$\sigma_{r_p} = \sigma_0 + (\sigma_{ax} - \sigma_0)\left(\frac{a_x}{r_p}\right)^{m+1}, \tag{10a}$$

$$\sigma_{\theta_p} = \sigma_0 - \frac{1}{m}(\sigma_{ax} - \sigma_0)\left(\frac{a_x}{r_p}\right)^{m+1}, \tag{10b}$$

$$u_{r_p} = \frac{(\sigma_{ax} - \sigma_0)}{2mG}\left(\frac{a_x}{r_p}\right)^{m+1} r_p. \tag{10c}$$

Subtracting equations (10a) and (10b), the following can be obtained:

$$\sigma_{r_p} - \sigma_{\theta_p} = \frac{m+1}{m}(\sigma_{ax} - \sigma_0)\left(\frac{a_x}{r_p}\right)^{m+1}. \tag{11}$$

According to the equation (4b), the deviator stress q_p at the elastic-plastic boundary for the cylindrical and spherical cases can be expressed as

$$q_p = \frac{\sqrt{m+2}}{2}\left(\sigma_{r_p} - \sigma_{\theta_p}\right). \tag{12}$$

Then, q_p can be calculated using the equations (11) and (12):

$$q_p = \frac{(m+1)\sqrt{m+2}}{2m}(\sigma_{ax} - \sigma_0)\left(\frac{a_x}{r_p}\right)^{m+1}. \tag{13}$$

Substituting equation (13) in equation (10a), the stresses σ_{r_p} at the elastic-plastic boundary can be obtained as

$$\sigma_{r_p} = \sigma_0 + \frac{2mq_p}{(m+1)\sqrt{m+2}}. \tag{14}$$

Similarly, the stresses σ_{θ_p} and displacement u_{r_p} at the elastic-plastic boundary can be expressed as

$$\sigma_{\theta_p} = \sigma_0 - \frac{2}{(m+1)\sqrt{m+2}} q_p, \tag{15a}$$

$$u_{r_p} = \frac{r_p\left(\sigma_{r_p} - \sigma_0\right)}{2mG} = \frac{1}{(m+1)\sqrt{m+2}}\left(\frac{r_p q_p}{G}\right). \tag{15b}$$

Using the conservation of volume, the boundary condition at the elastic-plastic boundary is

$$r_p^{m+1} - \left(r_p - u_{r_p}\right)^{m+1} = a_x^{m+1}. \tag{16}$$

Substituting equation (15b) in equation (16) leads to [15]

$$\frac{q_p}{G\sqrt{m+2}} = \left(\frac{r_p}{a_x}\right)^{-(m+1)}. \tag{17}$$

The soil in the plastic zone is analyzed by large strain theory and logarithmic strains are adopted. The strain coordination relationship is expressed as

$$\varepsilon_r = \ln\left(\frac{dr}{dr_0}\right), \tag{18a}$$

$$\varepsilon_\theta = \ln\left(\frac{r}{r_0}\right). \tag{18b}$$

The volumetric strain can be expressed as

$$\varepsilon_p = \varepsilon_r + m\varepsilon_\theta. \tag{19}$$

For the undrained condition, the volumetric strain, ε_p, is zero in the plastic zone, and the radial strain can be expressed as

$$\varepsilon_r = -m\varepsilon_\theta. \tag{20}$$

The boundary condition is obtained by conservation of volume:

$$r^{m+1} - r_0^{m+1} = a_x^{m+1}. \tag{21}$$

The yield function based on the modified Cambridge model can be expressed as [16]

$$f = q^2 - M^2\left[p'\left(p_y' - p'\right)\right] = 0, \tag{22}$$

where M is the slope of the critical state line, $M = 6\sin\varphi'/(3-\sin\varphi')$, φ' is the effective internal friction angle, and p_y' is the isotropic yield stress. At the elastic-plastic boundary, the average effective normal stress p_p', is found to be equal to the initial mean effective stress p_0', that is,

$$p_p' = p_0'. \tag{23}$$

Substituting equation (23) in equation (22), the deviator stress at the elastic-plastic boundary r_p is

$$q_p = Mp_0'\sqrt{R-1}, \tag{24}$$

where R is the isotropic overconsolidation ratio, defined $R = p_{y0}'/p_0'$ [17], and the pressure p_{y0}' is the maximum isotropic mean preconsolidation stress. For the isotropic consolidation condition, $R = \mathrm{OCR}$ [17].

In the plastic zone, the total volumetric strain is the sum of the elastic volumetric strain and the plastic volumetric strain. In the undrained loading process, the total volumetric strain is zero; that is,

$$\kappa\frac{dp'}{\nu p'} + (\lambda - \kappa)\frac{dp_y'}{\nu p_y'} = 0. \tag{25}$$

After integrating equation (25) and considering the relevant boundary conditions, the deviator stress q can be expressed as

$$q = Mp'\left[\mathrm{OCR}\left(\frac{p'}{p_0'}\right)^{-1/\Lambda} - 1\right]^{1/2}. \tag{26}$$

In the critical state $q = Mp'$, assuming that the shear modulus of the soil, G, is a constant, the ultimate deviatoric stress and undrained shear strength can be expressed as follows [15]:

$$q_u = Mp_u' = Mp_0'\left(\frac{\mathrm{OCR}}{2}\right)^{\Lambda}, \tag{27a}$$

$$s_u = \frac{q_u}{\sqrt{m+2}} = \frac{Mp_0'}{\sqrt{m+2}}\left(\frac{\mathrm{OCR}}{2}\right)^{\Lambda}. \tag{27b}$$

In the plastic zone, the difference between the deviator stress and the ultimate deviator stress is small. For the convenience of calculation, $q = q_u$ in the plastic zone is accepted. After considering the correlation differential relation and boundary conditions and integrating the equilibrium equation (3) and then combining equation (17), the radial stresses of the soil element in the plastic zone can be obtained [15]:

$$\sigma_r = \sigma_{r_p} + \frac{2mq_u}{\sqrt{m+2}}\ln\frac{r_p}{r}. \tag{28}$$

Figure 3 shows the relationship between normalized radial stress and radius for cylindrical ($m = 1$) and spherical ($m = 2$) cavity expansion.

It can be seen from Figure 3 that the radial stress of the cavity expansion increases with the increase in the degree of soil consolidation. For the same degree of consolidation of the soil, the radial stress in the spherical cavity expansion mode is higher than that in the cylindrical cavity expansion mode. When the cavity starts to expand from zero radius, the expansion problem has no length scale feature [18]. For the process of CPTU probe penetrating into the soil, the ultimate expanding pressure can be regarded as the expanding pressure when the cavity radius is the probe radius. That is, when $a_x = a$ and $r = a$, the ultimate expanding pressure can be obtained:

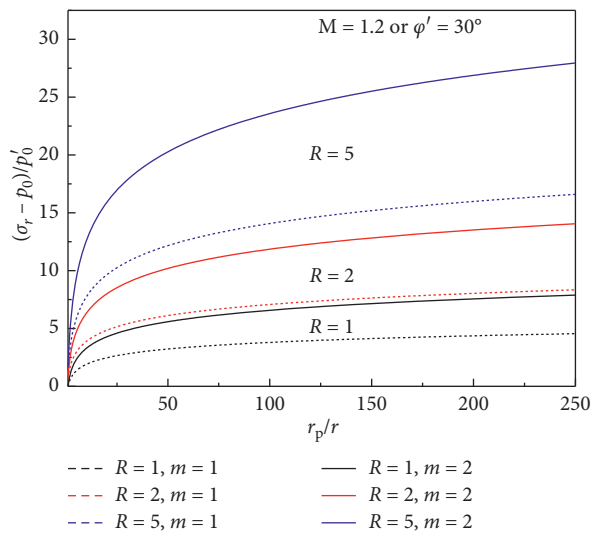

Figure 3: Relationship between normalized radial stress and radius.

$$\sigma_u = p_0 + \frac{m\sqrt{m+2}}{\sqrt{3^m}}(1 + \ln I_r)s_u. \tag{29}$$

2.2. Establishment of Overconsolidation Ratio Relation. In the CPTU test, the radius of the bottom of the probe is a, the angle of the cone tip is 2α, and the penetration resistance is q_t. It is assumed that the CPTU probe penetrates into the soil process is a cavity expansion which starts with a radius of zero, as shown in Figure 4. σ_u is the ultimate reaming pressure, and r_p is the radius of the elastoplastic boundary.

According to the similarity of the process of the probe penetrating into soil and the cavity expansion, in order to combine the cavity expansion pressure with the normal stress of the probe in the cavity expansion theory, the probe is simplified to a hemispherical cone with a radius of a. The probe cut into 1/2 circle by the horizontal plane of the cone bottom and the vertical plane of the diameter of the cone is taken as the research object. Because of its axial symmetry, 1/4 circle is taken for force analysis, as shown in Figure 5. The penetration resistance of the cone is q_t, the radius of the cone is a, and the normal and shear stress on the surface of the hemisphere are σ_n and τ_n, respectively.

After integrating the normal stress and the shear stress on the 1/4 arc, the equilibrium condition is as follows:

$$\begin{aligned} &\sum F_y = 0, \\ &q_t \cdot a = \int_0^a (\sigma \sin\theta + \tau \cos\theta) \cdot ds, \end{aligned} \tag{30}$$

where $ds = \sqrt{(1 + y'^2)}dx$, $\cos\theta = x/a$, and $\sin\theta = y/a$, and integrating and simplifying equation (30) leads to

$$q_t = \sigma_n + \tau_n. \tag{31}$$

When the cavity expanding radius reaches the CPTU probe radius a, the normal stress on the cone surface is equal to the ultimate expanding pressure of the cavity

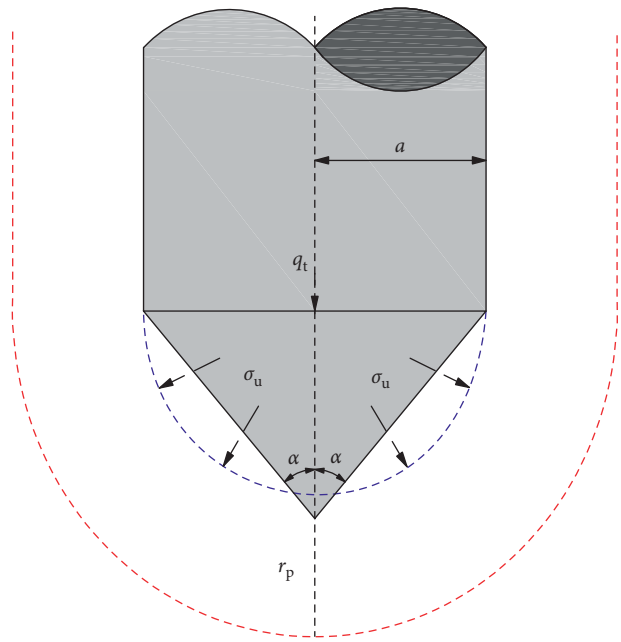

Figure 4: Assumed analysis model for piezocone penetration.

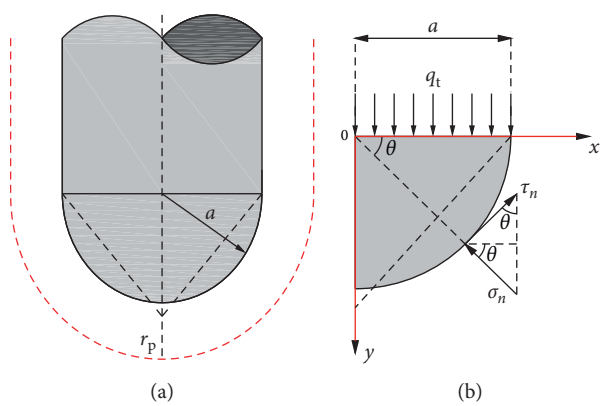

Figure 5: The diagram of cone force analysis.

expansion. The shear stress between the cone surface and the soil can be regarded as the contact friction between the cone and soil which can be expressed by the effective stress parameter [19]. The expression is shown in the following equation:

$$\tau_n = \sigma_n' \cdot \beta \cdot \tan\varphi' = (\sigma_n - u_m)\beta \cdot \tan\varphi', \tag{32}$$

where β is a friction factor between the surface of the cone and the soil, in the range of 0 to 1. In fact, it reflects the contact friction between the cone and the soil. The value of β is related to the material of the instrument and the type of soil [20]. When the surface of the steel is in contact with the clay and the silt, the friction factor is 0.6 and 0.7, respectively, and takes a value greater than or equal to 0.8 for saturated sand. For the marine soft clay of this research, it takes $\beta = 0.6$. φ' is the effective stress friction angle of the soil. u_m is the average pore pressure of the soil on the surface of the cone tip while the measured pore pressure of the probe u_2 is the pore pressure at the position

of the cone shoulder. According to reference [19], u_m cone can be expressed by the pore pressure u_2 at the position of the cone shoulder:

$$u_m = \lambda u_2, \tag{33}$$

where the parameter λ is related to the degree of consolidation of the soil, and the greater the degree of consolidation, the greater the value. In marine soft soil, it is a factor usually greater than unity which ranges from 1 to 1.1. Take $\lambda = 1$ for this research, which is based on reference [19]. From equations (31)–(33), cone tip resistance can be expressed as

$$q_t = \sigma_u + (\sigma_u - u_2)\beta \tan \varphi'. \tag{34}$$

The penetration process of the probe is actually a penetration mode between the expansion of the spherical and cylindrical cavity. In order to analyse the excess pore water pressure generated by the penetration process of the probe, the two modes are separately considered. The process of penetrating saturated soft soil at standard rate (2 cm/s) can be considered as an undrained loading process. When the cavity is expanded under undrained condition, the excess pore water pressure of the surrounding soil at the tip shoulder can be expressed as [15]

$$\Delta u = \frac{2m}{\sqrt{3^m}} S_u \ln\left(\frac{\sqrt{m+2}}{2} I_r\right) - \frac{2S_u}{M} + P_0', \tag{35}$$

where m is the parameter assigned $m = 1$ for the cylindrical case and $m = 2$ for the spherical case. For simplicity, it takes $P_0' = \sigma_{vo}'$.

By combining equations (27b) and (33)–(35), two prediction methods for OCR considering the influence of the cone roughness are obtained as follows:

(1) When $m = 1$, the prediction method for OCR based on the cylindrical cavity expansion mode is

$$\mathrm{OCR} = 2\left[\frac{1}{1+0.67M} \cdot \frac{q_t - 0.13(1+\beta\tan\varphi')p_0 - (0.87 - 0.13\beta\tan\varphi')u_2}{\sigma_{vo}'(1+\beta\tan\varphi')}\right]^{(1/\Lambda)}. \tag{36}$$

(2) When $m = 2$, the prediction method for OCR based on the spherical cavity expansion mode is

$$\mathrm{OCR} = 2\left[\frac{1}{1+0.67M} \cdot \frac{q_t - u_2}{\sigma_{vo}'(1+\beta\tan\varphi')}\right]^{(1/\Lambda)}. \tag{37}$$

2.3. Effect of Penetration Rate. Because of the characteristics of high moisture content, low shear strength, low permeability, and strong structure of marine soft clay, once disturbed, the strength of the soil will be weakened and the softening behavior will occur, and the strength change largely depends on the corresponding strain rate. The standard penetration rate of the CPTU test is 20 mm/s, and the strain rate of soil failure around the cone is much larger than the strain rate in the triaxial compression test conducted in the laboratory. As the shear rate increases, the undrained shear strength increases, so the effect of the strain rate difference on the undrained shear strength should be taken into consideration. Kulhawy and Mayne [21] proposed a modified relationship considering strain rate versus undrained shear strength through a number of experiments:

$$\frac{s_u}{(s_u)_{\dot{\varepsilon}=1\%/h}} = 1.0 + 0.1 \log \dot{\varepsilon}, \tag{38}$$

where $(s_u)_{\dot{\varepsilon}=1\%/h}$ is a reference value for undrained shear strength at a strain rate of $1\%/h$. s_u is the undrained shear strength at a strain rate of $\dot{\varepsilon}$.

According to Yu [18], the relationship between the radius rate $\dot{r}$ of the soil element around the cavity and the radial strain rate $\dot{a}$ of the cavity expansion is

$$\dot{r} = \left(\frac{a}{r}\right)^m \dot{a}, \tag{39}$$

$$\dot{\varepsilon}_r = -\frac{\partial \dot{r}}{\partial r} = \left(\frac{ma^m}{r^{m+1}}\right)\dot{a}. \tag{40}$$

For the soil element at the cavity wall $r = a$, the radial strain rate is

$$\dot{\varepsilon}_a = \frac{m}{a}\dot{a}. \tag{41}$$

The penetration rate can be approximately considered as $\dot{a}$. For a 10 cm^2 cone with a radius of 17.85 mm with the standard penetration rate 20 mm/s, the strain rate of soil element at cavity wall is about $\dot{\varepsilon}_a = 800000\%/h$ based on the spherical cavity expansion theory. And the undrained shear strength interpreted from the piezocone test is 59% larger than that determined from the consolidated undrained triaxial test with the reference strain rate calculated from equation (38), which is consistent with the study of the scholar Chang et al. [22]. The rate of shearing in the consolidated undrained (CU) triaxial test is usually chosen based on the pore water pressure equilibrium condition of the soil sample during the shearing process. The rate is typically 0.5% per hour for clays in the CU test. And the ratio of the undrained shear strength $(s_u)_{CUTC}$, at 0.5% per hour, to the reference value $(s_u)_{\dot{\varepsilon}=1\%/h}$ is 0.97. Assuming that the strain rate factor of the soil around the cone is $\alpha_\varepsilon = (s_u)_{cptu}/(s_u)_{CUTC}$, the strain rate factors with different types of CPTU probes at standard penetration rate 20 mm/s are shown in Table 1.

After considering the effect of strain rate, the undrained shear strength in equation (27b) can be expressed as

Table 1: α_ε with different types of CPTU probes.

Probe types	Cavity expansion mode	$(s_u)_{cptu}/((s_u)_{\dot{\varepsilon}=1\%/h})$	$\alpha_\varepsilon = (s_u)_{cptu}/((s_u)_{CUTC})$
$10\,cm^2$	Spherical	1.59	1.64
	Cylindrical	1.56	1.61
$15\,cm^2$	Spherical	1.58	1.63
	Cylindrical	1.55	1.60

$$s_u = \alpha_\varepsilon \cdot \frac{M p_0'}{\sqrt{m+2}} \left(\frac{\mathrm{OCR}}{2}\right)^{\Lambda}. \tag{42}$$

After considering the influence of the difference in strain rate of the soil between probe penetration process and triaxial compression test on undrained shear strength, the OCR prediction method considering the influence of cone roughness and cone penetration rate can be obtained.

(1) When $m = 1$, the OCR prediction method based on the cylindrical cavity expansion mode can be expressed as (Method 1)

$$\mathrm{OCR} = 2\left[\frac{1}{1+0.67M} \cdot \frac{q_t - 0.13(1+\beta\tan\varphi')p_0 - (0.87 - 0.13\beta\tan\varphi')u_2}{\alpha_\varepsilon \sigma_{vo}'(1+\beta\tan\varphi')}\right]^{(1/\Lambda)}. \tag{43}$$

(2) When $m = 2$, the OCR prediction method based on the spherical cavity expansion mode can be expressed as (Method 2)

$$\mathrm{OCR} = 2\left[\frac{1}{1+0.67M} \cdot \frac{q_t - u_2}{\alpha_\varepsilon \sigma_{vo}'(1+\beta\tan\varphi')}\right]^{(1/\Lambda)}. \tag{44}$$

3. Case Studies

3.1. Comparisons of OCR Obtained from Two Methods Proposed in This Paper and Existing Methods Based on CPTU. To validate the methods proposed in this paper, the predictions of equations (43) and (44) were compared with the results of in situ CPTU tests for marine soft clay in two coastal areas [23, 24]. Moreover, the predictions of Wayne's method [12] and Chanmee's method [14] were also included in comparison with further interpretation of the reliability and superiority of the methods proposed in this paper. Table 2 lists the model input parameters used in the analyses. It is noted that the type of probes is adopted as a cone with an angle of 60° and a cone bottom area of $10\,cm^2$ and the penetration rate is 2 cm/s by default in the selected in situ CPTU tests. Since the piezocone probe is generally a steel material, the friction factor β here is taken as 0.6. For structurally sensitive marine soft clays, the plastic volumetric strain rate Λ is 1.0 [25].

3.1.1. Location 1: Busan, South Korea. Singh and Chung [23] conducted a CPTU test at two test sites in the Midwest Plain of the Luodong Delta in Busan. The surface of the two test points is about 4 m thick silty sand and then deep silt or silty soft soil. The basic physical properties of the soil at the two test points are about the same. The test data of test site D2 are selected as the citation in this paper. The average effective internal friction angle of soft soil is $\varphi' = 29°$, and the water content is between 50% and 85%. The plasticity index is about 30 and decreases when the depth increases. The measured OCR varies from 1.2 to 2.05. The CPTU probe of the test has a cone tip angle of 60° and a cone bottom area of $15\,cm^2$. The predicted values of OCR obtained by the four methods are compared with the measured values, as shown in Figure 6.

3.1.2. Location 2: St. Marcel, Canada. St. Marcel is located along the St. Lawrence River in Montana, southern Canada. Lefebvre and Langlois [24] reported that the surface of the soil layer is 1.5 m fully weathered silty clay, and the lower layer is a deep sedimentary light gray soft clay with a natural moisture content of about 80%, which is 15%–20% higher than the liquid limit. The overconsolidation ratio is 1.8 at a depth of 2 meters, which decreases slightly with increasing depth and reaches a constant value of 1.3 at 7 meters under the ground surface [19]. The predicted values of OCR obtained by the four methods were compared with the measured values, as shown in Figure 7.

From Figures 6 and 7, it can be seen that the four prediction methods based on CPTU can well describe the variation trend of measured values of OCR. At the soil interface, all four prediction methods for OCR show the deviations to some extent, which may be caused by the fluctuation of CPTU test results (q_t and u_2) due to the influence of interface effect. Although there are deviations, two proposed predictions in this paper show great applicability and rationality in general. Compared with Chanmee's method and Wayne's method, the predicted values of Method 2 is smaller than that of Chanmee's method and Method 1, and the predicted values of Chanmee's method and Method 1 is smaller than that of Wayne's method.

In order to compare the prediction accuracy between the two proposed prediction methods, Wayne's method and

Table 2: Information summary of test input parameters.

Locations	References	Input parameters					
		β	Λ	Cone tip angle	Cone bottom area	N_{kt}	Internal friction angle of soil
Busan, South Korea	Singh and Chung [23]	0.6	1.0	60°	15 cm^2	11.0	29°
St. Marcel, Canada	Lefebvre and Langlois [24]	0.6	1.0	60°	10 cm^2	11.25	26°

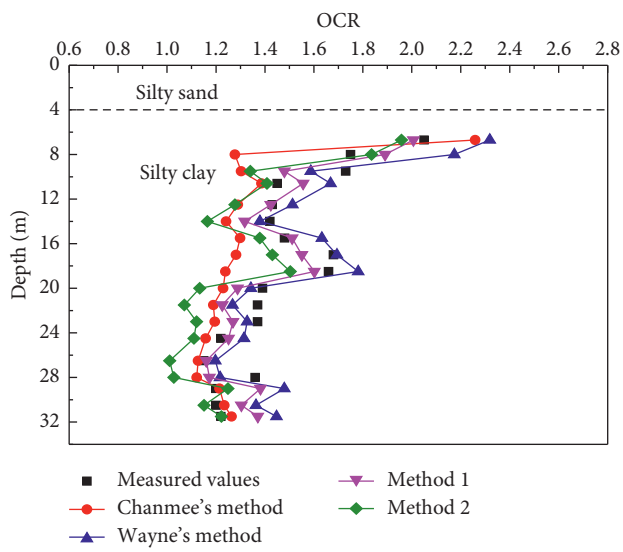

Figure 6: The predicted values of OCR by four methods for Busan site in Korea based on CPTU.

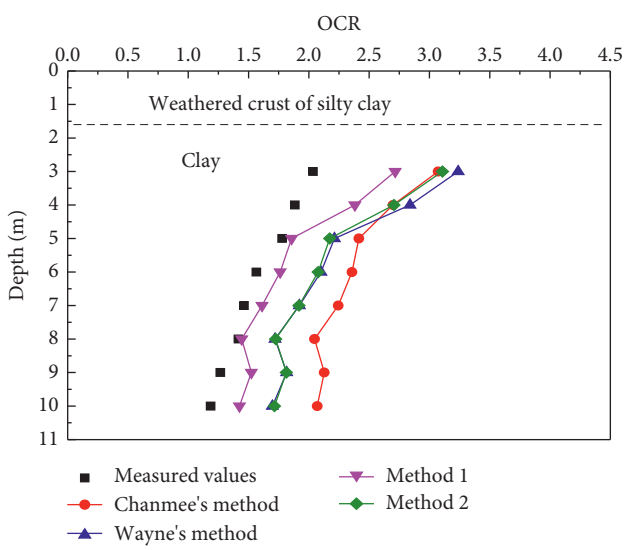

Figure 7: The predicted values of OCR by four methods for St. Marcel site in Canada based on CPTU.

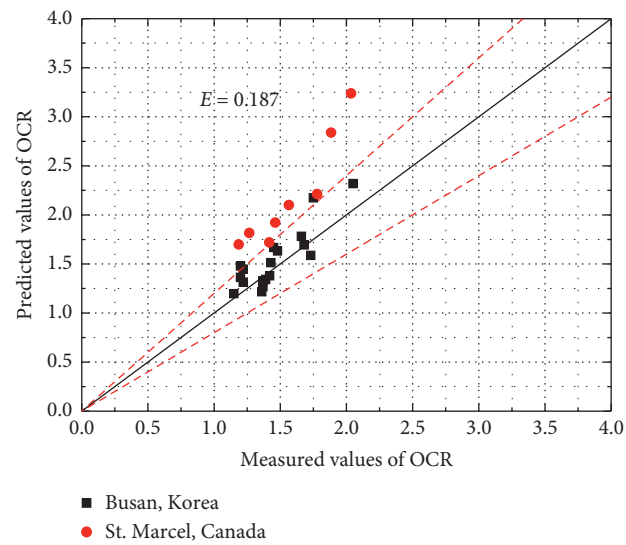

Figure 8: Comparison of the measured values and predicted values of the OCR using Wayne's method.

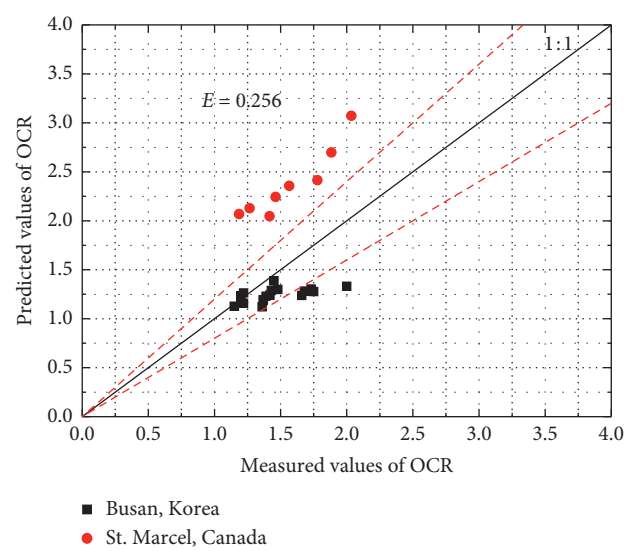

Figure 9: Comparison of the measured values and predicted values of the OCR using Chanmee's method.

Chanmee's method, which are based on the CPTU test, more intuitively, the prediction values of OCR of the two test sites are compared with the measured datum in the graph with the measured values of OCR as the horizontal axis and the predicted values of OCR as the vertical axis as shown in Figures 8–11. Firstly, the overall scatter of the prediction methods is analyzed. A reference line with an accuracy of 80% is introduced on the upper and lower sides of the 1 : 1 diagonal, and the points in the two reference lines have an accuracy of more than 80%. Secondly, the relative error is introduced to quantify and refine the scatter of the four OCR prediction methods:

$$E = \frac{1}{n}\sum_{i}\frac{\left|\mathrm{OCR_p} - \mathrm{OCR}_m\right|}{\mathrm{OCR}_m}, \tag{45}$$

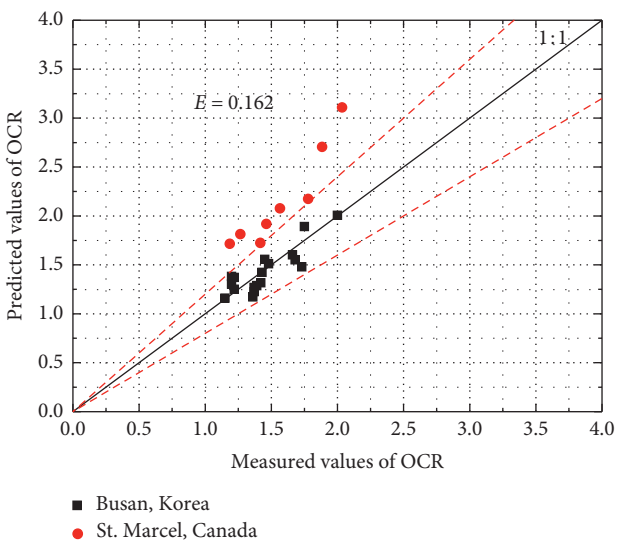

Figure 10: Comparison of the measured values and predicted values of the OCR using Method 1.

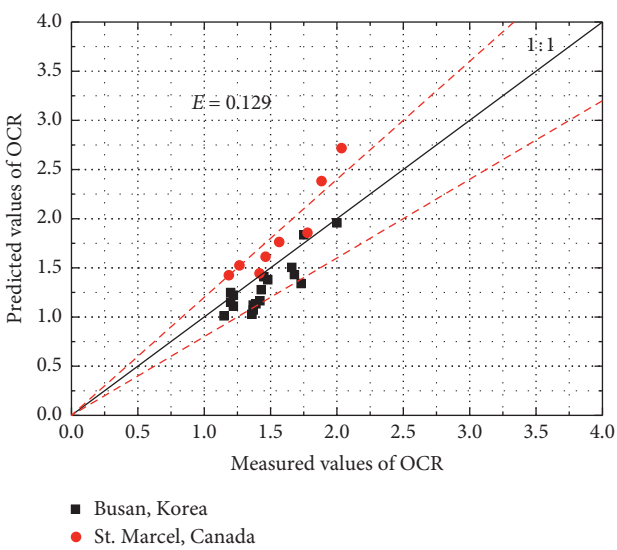

Figure 11: Comparison of the measured values and predicted values of the OCR using Method 2.

where OCR_p is the predicted value of a method OCR, OCR_m is the measured value of OCR, and n is the total number of data points.

The data distribution of four methods in the zone of 80% accuracy and the relative error can be obtained by Figures 8–11. And the results are shown in Table 3, which shows the following: (a) When the error between the predicted value of the OCR and the measured value does not exceed 20%, Method 2 has a higher assurance indicating higher accuracy. (b) The relative error between two proposed prediction methods and Wayne's method is close, and smaller than that of Chanmee's method, showing smaller discreteness. (c) In terms of comparing the predicted value with the measured value, the data are above the 1 : 1 diagonal, indicating that the prediction method is overestimated, while it indicates that the prediction method is underestimated when the data are below the 1 : 1 diagonal. The four methods show a certain over- or underestimation under different consolidation degrees of soil. In order to improve the applicability in different cases of the OCR predictions, the average values of the two proposed methods are recommended as reference value for the OCR of marine soft soil.

Table 3: Analysis and comparison results of four methods.

Methods		Items	
		Within the zone of 80% accuracy (%)	Relative error
CPTU	Wayne's method	69	0.187
	Chanmee's method	46	0.256
	Method 1	73	0.162
	Method 2	85	0.129

3.2. Comparisons of OCR Based on CPTU (Proposed Methods in This Paper), DMT, and FVT. According to reference [23], Singh and Chung conducted three in situ tests at D2 test site in Busan Korea, namely, CPTU, DMT (flat dilatometer test), and FVT (field vane test), respectively. The comparisons of the predicted OCR using CPTU, DMT, and FVT can further verify the applicability of the methods for predicting OCR based on CPTU proposed in this paper. Figure 12 shows the predicted values of OCR based on CPTU, DMT, and FVT for D2 test site. The results show that the predicted values of OCR using CPTU, DMT, and FVT at D2 test site are in good agreement with the measured values. At the same time, the three in situ test methods show some similarities in describing the trend of OCR, which indicates that the methods proposed in this paper based on CPTU is applicable to marine soft soil.

4. Conclusions

In this paper, the CPTU cone head is assumed to be a hemispherical cone head considering the penetration mechanism of CPTU. Moreover, the compaction modes of CPTU probe penetrating into soil are adopted as spherical and cylindrical cavity expansion modes, respectively. The ultimate expansion pressures of probe penetrating into soil under the spherical and cylindrical cavity expansion modes are firstly obtained by virtue of the theory of cavity expansion. Then, two prediction methods for OCR considering the roughness and penetration rate of cone are proposed by combining the ultimate expansion pressures of probe penetrating with the approximate closed solution of cavity expansion in the modified Cambridge model, which is suitable for predicting the OCR of marine soft clay. Finally, to verify the reliability of the two proposed prediction methods, comparisons with the in situ CPTU tests of marine soft clay in two coastal areas and two existing prediction methods are performed. The main conclusions are as follows:

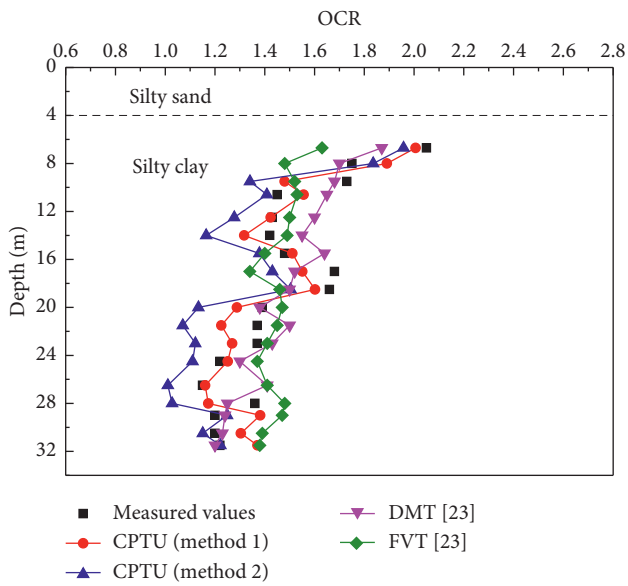

Figure 12: The predicted values of OCR based on CPTU, DMT, and FVT for D2 test site in Busan, South Korea.

(1) From the penetration mechanism of CPTU, it can be seen that the process of penetration of the CPTU probe into soil can be regarded as the process of cavity expansion from zero radius, and the radial stress increases with the increase of consolidation degree of soil. Under the same conditions, the radial stress of spherical cavity expansion mode is about 1.7 times compared with cylindrical cavity expansion mode.

(2) Two new methods proposed in this paper have better accuracy in predicting the OCR value of marine soft clay in general, with higher assurance rate within 80% of the prediction accuracy, which can better describe the trend of the OCR value of marine soft clay along with the depth.

(3) The comparative results show that predictions of OCR of marine soft clay in this paper are close to Wayne's method and more accurate than Chanmee's method since the factors such as cone roughness and penetration rate are considered in the new proposed prediction methods. In order to improve the applicability in different cases of the OCR predictions, the average values of two proposed methods are recommended as a reference value for the OCR of marine soft soil.

Data Availability

An executable file to calculate the two prediction methods for OCR is available from the corresponding author upon request.

Conflicts of Interest

The authors declare that they have no conflicts of interest.

Acknowledgments

This work was supported by the National Natural Science Foundation of China (grant no. 51678363), Shenzhen Science and Technology Project (no. JCYJ20150525092941052), and Underground Engineering (Tongji University) (no. KLE-TJGE-B0905).

References

[1] I. Guettaya and M. R. E. Ouni, "In situ-based assessment of soil liquefaction potential-case study of an earth dam in Tunisia," *Frontiers of Structural and Civil Engineering*, vol. 8, no. 4, pp. 456–461, 2014.

[2] P. Samui, "Liquefaction prediction using support vector machine model based on cone penetration data," *Frontiers of Structural and Civil Engineering*, vol. 7, no. 1, pp. 72–82, 2013.

[3] A. Sara, "Prediction of the shear wave velocity V_S from CPT and DMT at research sites," *Frontiers of Structural and Civil Engineering*, vol. 8, no. 1, pp. 83–92, 2014.

[4] D. C. F. Lo Presti, M. Maugeri, A. Cavallaro, and O. Pallara, "Shear modulus and damping of a stiff clay from in situ and laboratory tests," in *Proceedings of the 1st International Conference on Site Characterization*, pp. 1293–1300, Atlanta, GA, USA, April 1998.

[5] S. Y. Liu, G. J. Cai, and L. Y. Tong, *Theory and Engineering Application of Modern Multifunctional CPTU Technology*, Science Press, Beijing, China, 2013, in Chinese.

[6] P. W. Mayne, "Stress-strain-strength-flow parameters from enhanced in situ tests," in *Proceedings of International Conference on In Situ Measurement of Soil Properties and Case Histories*, pp. 27–48, Bali, Indonesia, May 2001.

[7] P. W. Mayne, "CPT indexing of in situ OCR in clays," in *Proceedings of the International Conference on in Use of In Situ Tests in Geotechnical Engineering*, ASCE, Blacksburg, VA, USA, 2015.

[8] C. P. Wroth, "Penetration testing-A more rigorous approach to interpretation," in *Proceedings of the International Conference on Penetration Testing*, pp. 303–311, Balkema, Rotterdam, Netherlands, 1988.

[9] B. S. Chen and P. W. Mayne, "Statistical relationships between piezocone measurements and stress history of clays," *Canadian Geotechnical Journal*, vol. 33, no. 3, pp. 488–498, 1996.

[10] L. Y. Tong, G. J. Cai, S. Y. Liu, and G. Y. Du, "Use of piezocone tests to predict consolidation yield stress and overconsolidation ratio of lagoonal deposit soil," *Journal of Southeast University*, vol. 23, no. 1, pp. 112–116, 2007.

[11] G. T. Houlsby, "Piezocone penetration test," in *Proceedings of the Geotechnology Conference on Penetration Testing in the UK*, pp. 141–146, Birmingham, UK, July 1988.

[12] P. W. Mayne, "Determination of OCR in clays by piezocone tests using cavity expansion and critical state concepts," *Soils and Foundations*, vol. 31, no. 2, pp. 65–76, 1991.

[13] Y. G. Zhang, J. P. Li, and Z. P. Hu, "A modified approach to determine over consolidation ration from piezocone penetration tests in soft clays," *Chinese Journal of Rock Mechanics and Engineering*, vol. 36, no. 6, 2017, in Chinese.

[14] N. Chanmee, J. Chai, T. Hino, and J. Wang, "Methods for evaluating overconsolidation ratio from piezocone sounding results," *Underground Space*, vol. 2, no. 3, pp. 182–194, 2017.

[15] L. F. Cao, C. I. Teh, and M. F. Chang, "Undrained cavity expansion in modified cam clay I: theoretical analysis," *Géotechnique*, vol. 51, no. 4, pp. 323–334, 2001.

[16] D. M. Wood, *Soil Behaviour and Critical State Soil Mechanics*, Cambridge University Press, Cambridge, UK, 1991.
[17] C. P. Wroth, "The interpretation of in situ soil tests," *Géotechnique*, vol. 34, no. 4, pp. 449–489, 1984.
[18] H. S. Yu, *Cavity Expansion Methods in Geomechanics*, Springer, Dordrecht, Netherlands, 2000.
[19] J.-M. Konrad and K. T. Law, "Preconsolidation pressure from piezocone tests in marine clays," *Géotechnique*, vol. 37, no. 2, pp. 177–190, 1987.
[20] J. G. Potyondy, "Skin friction between various soils and construction materials," *Géotechnique*, vol. 11, no. 4, pp. 339–353, 1961.
[21] F. H. Kulhawy and P. W. Mayne, "Manual on estimating soil properties for foundation design," Report EL-6800, Electric Power Research Institute, Palo Alto, CA, USA, 1990.
[22] M. F. Chang, C. I. Teh, and L. F. Cao, "Undrained cavity expansion in modified cam clay II: application to the interpretation of cone penetration tests," *Géotechnique*, vol. 51, no. 4, pp. 335–350, 2001.
[23] V. K. Singh and S. G. Chung, "Evaluation of overconsolidation ratios from laboratory and in situ tests on busan clay," *Engineering Geology*, vol. 199, pp. 38–47, 2015.
[24] G. Lefebvre and P. Langlois, "Observation of la fissuration des argiles pair claquage hydraulique sites Saint Marcel and Ottawa," Report, Division of Building Research, National Research Council of Canada, Ottawa, Canada, 1982.
[25] D. N. Brow and P. W. Mayne, "Stress history profiling of marine clays by piezoncone," in *Proceedings of the 4th Canadian Conference on Marine Geotechnical Engineering*, pp. 176–191, St. John's, Newfoundland, Canada, 1993.